Progress In Electromagnetics Research, Vol. 122, 175–196, 2012

REDUCTION OF NUMERICAL DISPERSION OF THE SIX-STAGES SPLIT-STEP UNCONDITIONALLY-STABLE FDTD METHOD WITH CONTROLLING PARAMETERS

Y.-D. Kong[1] and Q.-X. Chu[1, 2, *]

[1]School of Electronic and Information Engineering, South China University of Technology, Guangzhou, Guangdong 510640, China

[2]The State Key Laboratory of Millimeter Waves, Nanjing, Jiangsu 210096, China

Abstract—A new approach to reduce the numerical dispersion of the six-stages split-step unconditionally-stable finite-difference time-domain (FDTD) method is presented, which is based on the split-step scheme and Crank-Nicolson scheme. Firstly, based on the matrix elements related to spatial derivatives along the x, y, and z coordinate directions, the matrix derived from the classical Maxwell's equations is split into six sub-matrices. Simultaneously, three controlling parameters are introduced to decrease the numerical dispersion error. Accordingly, the time step is divided into six sub-steps. Secondly, the analysis shows that the proposed method is unconditionally stable. Moreover, the dispersion relation of the proposed method is carried out. Thirdly, the processes of determination of the controlling parameters are shown. Furthermore, the dispersion characteristics of the proposed method are also investigated, and the maximum dispersion error of the proposed method can be decreased significantly. Finally, numerical experiments are presented to substantiate the efficiency of the proposed method.

1. INTRODUCTION

The finite-difference time-domain (FDTD) method [1] has been proven to be an established numerical technique that provides accurate predictions of field behaviors for electromagnetic interaction problems [2–11]. Some enhanced FDTD methods have been

Received 25 August 2011, Accepted 7 November 2011, Scheduled 17 November 2011

* Corresponding author: Qing-Xin Chu (qxchu@scut.edu.cn).

proposed [12–18]. However, the conventional FDTD method is an explicit method, and the time step size is constrained by the Courant-Friedrichs-Lewy (CFL) condition [19], which affects its computational efficiency when fine meshes are required.

Recently, to overcome the CFL condition on the time step size of the FDTD method, an unconditionally-stable FDTD method based on the alternating direction implicit (ADI) technique was developed [20, 21]. The ADI-FDTD method has second-order accuracy both in time and space. Nevertheless, it presents large numerical dispersion error with large time steps. To improve the dispersion performance, several methods were proposed, such as parameter-optimized [22, 23], artificial-anisotropy methods [24–26] and the simplified sampling biorthogonal ADI method [27].

The Crank-Nicolson (CN) scheme is unconditionally-stable and is believed to have high numerical accuracy [19]. However, spatial discretization leads to a huge spare irreducible matrix. Directly solving the matrix by Gaussian elimination or an iterative method is so CPU intensive that the CN scheme is hardly unstable for practical problems. CN-based FDTD methods [28–36] use factorization-splitting and are fractional-step, split-step, or sub-step methods, leading to simple matrices at each sub-step, usually tri-diagonal if second-order differencing is used. Particularly, the Crank-Nicolson-Douglas-Gunn (CNDG) method as two-dimensional (2-D) [28], the Crank-Nicolson cycle-sweep (CNCS) method in 2-D [29] and as in 3-D [30], and the Crank-Nicolson approximate-factorization-splitting (CNAFS) method in 3-D [31] have small anisotropy, and the Crank-Nicolson direct-splitting (CNDS) method in 3-D [32].

Along the same line, other unconditionally-stable methods such as split-step [37–47] and locally-one dimensional (LOD) [48–52] FDTD methods were developed. Specially, the two sub-steps method in [37], the three sub-steps methods in [38–40], the four sub-steps methods in [41–44] and six sub-steps methods in [45–47]. The LOD-FDTD method can be considered as a split-step approach (SS1) with first-order accuracy in time, which consumes less CPU time than that of the ADI-FDTD method. Particularly, The LOD-FDTD methods in 2-D [48, 49], and 3-D LOD-FDTD methods with a three-step scheme [50] and a two-step scheme [51]. The method in [47] is based on the split-step scheme and Crank-Nicolson scheme, and denoted as SSCN6-FDTD herein. The SSCN6-FDTD method has second-order accuracy both in time and space, and has simpler procedure formulation than those of the ADI-FDTD method and the LOD-FDTD method. However, when the size of time step is larger, the numerical dispersion error of the SSCN6-FDTD method is becoming larger.

To reduce the numerical dispersion error further, an efficient SSCN6-FDTD method in 3-D domains with controlling parameters is presented in this paper. Firstly, based on the matrix elements related to spatial derivatives along the x, y, and z coordinate directions, the Maxwell's matrix is split into six sub-matrices. Simultaneously, three controlling parameters are introduced to decrease the numerical dispersion error. Accordingly, the time step is divided into six sub-steps, and the proposed method is denoted by E-SSCN6-FDTD. Secondly, the proposed method is proven to be unconditionally stable by using the Fourier method. Furthermore, the dispersion relation of the proposed method is carried out. Thirdly, the processes of determination of the controlling parameters are shown. Moreover, the dispersion characteristics of the proposed method also are investigated, and the maximum dispersion error of the proposed method is lower than those of the SSCN6-FDTD method, the CNDS-FDTD method, the CNAFS-FDTD method, and the LOD-FDTD method. Finally, numerical experiments are presented, which can be concluded that the numerical dispersion error of the proposed method can be decreased significantly.

2. FORMULATION OF THE E-SSCN6-FDTD METHOD

In linear, isotropic, non-dispersive and lossless medium, ε and μ are the electric permittivity and magnetic permeability, respectively. Then, the 3-D Maxwell's equations can be written in a matrix form as

$$\frac{\partial \vec{u}}{\partial t} = [M]\,\vec{u} \tag{1}$$

where $\vec{u} = [E_x, E_y, E_z, H_x, H_y, H_z]^T$, and $[M]$ is the Maxwell's matrix as below.

Based on the matrix elements related to spatial derivatives along the x, y, and z coordinate directions, the Maxwell's matrix is split into six sub-matrices, $[D_1]$, $[E_1]$, $[F_1]$, $[D_2]$, $[E_2]$, and $[F_2]$. Simultaneously, three controlling parameters of C_x, C_y, and C_z are introduced to decrease the numerical dispersion error.

$$[M] = \begin{bmatrix} 0 & 0 & 0 & 0 & -\frac{1}{\varepsilon}\frac{\partial}{\partial z} & \frac{1}{\varepsilon}\frac{\partial}{\partial y} \\ 0 & 0 & 0 & \frac{1}{\varepsilon}\frac{\partial}{\partial z} & 0 & -\frac{1}{\varepsilon}\frac{\partial}{\partial x} \\ 0 & 0 & 0 & -\frac{1}{\varepsilon}\frac{\partial}{\partial y} & \frac{1}{\varepsilon}\frac{\partial}{\partial x} & 0 \\ 0 & \frac{1}{\mu}\frac{\partial}{\partial z} & -\frac{1}{\mu}\frac{\partial}{\partial y} & 0 & 0 & 0 \\ -\frac{1}{\mu}\frac{\partial}{\partial z} & 0 & \frac{1}{\mu}\frac{\partial}{\partial x} & 0 & 0 & 0 \\ \frac{1}{\mu}\frac{\partial}{\partial y} & -\frac{1}{\mu}\frac{\partial}{\partial x} & 0 & 0 & 0 & 0 \end{bmatrix} \tag{2}$$

$$[D_1]=\begin{bmatrix}0&0&0&0&0&0\\0&0&0&0&0&0\\0&0&0&0&\frac{1}{\varepsilon}\frac{\partial}{\partial x}&0\\0&0&0&0&0&0\\0&0&\frac{1}{\mu}\frac{\partial}{\partial x}&0&0&0\\0&0&0&0&0&0\end{bmatrix}\quad [D_2]=\begin{bmatrix}0&0&0&0&0&0\\0&0&0&0&0&-\frac{1}{\varepsilon}\frac{\partial}{\partial x}\\0&0&0&0&0&0\\0&0&0&0&0&0\\0&0&0&0&0&0\\0&-\frac{1}{\mu}\frac{\partial}{\partial x}&0&0&0&0\end{bmatrix}$$

$$[E_1]=\begin{bmatrix}0&0&0&0&0&\frac{1}{\varepsilon}\frac{\partial}{\partial y}\\0&0&0&0&0&0\\0&0&0&0&0&0\\0&0&0&0&0&0\\0&0&0&0&0&0\\\frac{1}{\mu}\frac{\partial}{\partial y}&0&0&0&0&0\end{bmatrix}\quad [E_2]=\begin{bmatrix}0&0&0&0&0&0\\0&0&0&0&0&0\\0&0&0&-\frac{1}{\varepsilon}\frac{\partial}{\partial y}&0&0\\0&0&-\frac{1}{\mu}\frac{\partial}{\partial y}&0&0&0\\0&0&0&0&0&0\\0&0&0&0&0&0\end{bmatrix} \tag{3}$$

$$[F_1]=\begin{bmatrix}0&0&0&0&0&0\\0&0&0&\frac{1}{\varepsilon}\frac{\partial}{\partial z}&0&0\\0&0&0&0&0&0\\0&\frac{1}{\mu}\frac{\partial}{\partial z}&0&0&0&0\\0&0&0&0&0&0\\0&0&0&0&0&0\end{bmatrix}\quad [F_2]=\begin{bmatrix}0&0&0&0&-\frac{1}{\varepsilon}\frac{\partial}{\partial z}&0\\0&0&0&0&0&0\\0&0&0&0&0&0\\0&0&0&0&0&0\\-\frac{1}{\mu}\frac{\partial}{\partial z}&0&0&0&0&0\\0&0&0&0&0&0\end{bmatrix}$$

Then, (1) can be written as

$$\frac{\partial \vec{u}}{\partial t}=C_x\cdot[D_1]\vec{u}+C_y\cdot[E_1]\vec{u}+C_z\cdot[F_1]\vec{u}+C_x\cdot[D_2]\vec{u}+C_y\cdot[E_2]\vec{u}+C_z\cdot[F_2]\vec{u} \tag{4}$$

By using the split-step scheme [37], (4) is divided into six sub-equations, from n to $n+1$, one time step is divided into six sub-steps accordingly, $n \to n+1/6$, $n+1/6 \to n+2/6$, $n+2/6 \to n+3/6$, $n+3/6 \to n+4/6$, $n+4/6 \to n+5/6$, and $n+5/6 \to n+1$, by successively solving

$$\text{sub-step1}: \quad \frac{\partial \vec{u}}{\partial t}=6\cdot C_x\cdot[D_1]\,\vec{u} \quad n \to n+1/6 \tag{5a}$$

$$\text{sub-step2}: \quad \frac{\partial \vec{u}}{\partial t}=6\cdot C_y\cdot[E_1]\,\vec{u} \quad n+1/6 \to n+2/6 \tag{5b}$$

$$\text{sub-step3}: \quad \frac{\partial \vec{u}}{\partial t}=6\cdot C_z\cdot[F_1]\,\vec{u} \quad n+2/6 \to n+3/6 \tag{5c}$$

$$\text{sub-step4}: \quad \frac{\partial \vec{u}}{\partial t}=6\cdot C_x\cdot[D_2]\,\vec{u} \quad n+3/6 \to n+4/6 \tag{5d}$$

$$\text{sub-step5}: \quad \frac{\partial \vec{u}}{\partial t}=6\cdot C_y\cdot[E_2]\,\vec{u} \quad n+4/6 \to n+5/6 \tag{5e}$$

$$\text{sub-step6}: \quad \frac{\partial \vec{u}}{\partial t}=6\cdot C_z\cdot[F_2]\,\vec{u} \quad n+5/6 \to n+1 \tag{5f}$$

Furthermore, the right side of the above equations can be approximated

by using the Crank-Nicolson scheme [28]. Subsequently, six sub-procedures are generated as follows

$$\left([I]-\frac{\Delta t}{2}\cdot C_x\cdot[D_1]\right)\vec{u}^{\,n+1/6}=\left([I]+\frac{\Delta t}{2}\cdot C_x\cdot[D_1]\right)\vec{u}^{\,n} \tag{6a}$$

$$\left([I]-\frac{\Delta t}{2}\cdot C_y\cdot[E_1]\right)\vec{u}^{\,n+2/6}=\left([I]+\frac{\Delta t}{2}\cdot C_y\cdot[E_1]\right)\vec{u}^{\,n+1/6} \tag{6b}$$

$$\left([I]-\frac{\Delta t}{2}\cdot C_z\cdot[F_1]\right)\vec{u}^{\,n+3/6}=\left([I]+\frac{\Delta t}{2}\cdot C_z\cdot[F_1]\right)\vec{u}^{\,n+2/6} \tag{6c}$$

$$\left([I]-\frac{\Delta t}{2}\cdot C_x\cdot[D_2]\right)\vec{u}^{\,n+4/6}=\left([I]+\frac{\Delta t}{2}\cdot C_x\cdot[D_2]\right)\vec{u}^{\,n+3/6} \tag{6d}$$

$$\left([I]-\frac{\Delta t}{2}\cdot C_y\cdot[E_2]\right)\vec{u}^{\,n+5/6}=\left([I]+\frac{\Delta t}{2}\cdot C_y\cdot[E_2]\right)\vec{u}^{\,n+4/6} \tag{6e}$$

$$\left([I]-\frac{\Delta t}{2}\cdot C_z\cdot[F_2]\right)\vec{u}^{\,n+1}=\left([I]+\frac{\Delta t}{2}\cdot C_z\cdot[F_2]\right)\vec{u}^{\,n+5/6} \tag{6f}$$

where $[I]$ is a 6×6 identity matrix. Without loss of generality, the updating equations are herein presented for the sub-step 1 only. More specifically, (6a) can be rewritten as

$$\text{sub-step1}: \quad E_z^{n+1/6}=E_z^n+C_x\cdot\frac{\Delta t}{2\varepsilon}\cdot\frac{\partial}{\partial x}\left(H_y^{n+1/6}+H_y^n\right) \tag{7a}$$

$$H_y^{n+1/6}=H_y^n+C_x\cdot\frac{\Delta t}{2\mu}\cdot\frac{\partial}{\partial x}\left(E_z^{n+1/6}+E_z^n\right) \tag{7b}$$

By substituting (7b) into (7a), the following tri-diagonal equations can be generated

$$\begin{aligned}&\left[1+\frac{(C_x\Delta t)^2}{2\varepsilon\mu\,(\Delta x)^2}\right]E_z\Big|_{i,j,k+1/2}^{n+1/6}-\frac{(C_x\Delta t)^2}{4\varepsilon\mu\,(\Delta x)^2}\left(E_z\Big|_{i+1,j,k+1/2}^{n+1/6}+E_z\Big|_{i-1,j,k+1/2}^{n+1/6}\right)\\&=\left[1-\frac{(C_x\Delta t)^2}{2\varepsilon\mu(\Delta x)^2}\right]E_z\Big|_{i,j,k+1/2}^{n}+\frac{(C_x\Delta t)^2}{4\varepsilon\mu(\Delta x)^2}\left(E_z\Big|_{i+1,j,k+1/2}^{n}+E_z\Big|_{i-1,j,k+1/2}^{n}\right)\\&+\frac{C_x\Delta t}{\varepsilon\Delta x}\left(H_y\Big|_{i+1/2,j,k+1/2}^{n}-H_y\Big|_{i-1/2,j,k+1/2}^{n}\right)\end{aligned} \tag{8}$$

Moreover, (7b) can be explicitly solved by

$$\begin{aligned}H_y\Big|_{i+1/2,j,k+1/2}^{n+1/6}&=H_y\Big|_{i+1/2,j,k+1/2}^{n}+\frac{C_x\Delta t}{2\mu\Delta x}\left(E_z\Big|_{i+1,j,k+1/2}^{n+1/6}\right.\\&\left.-E_z\Big|_{i,j,k+1/2}^{n+1/6}+E_z\Big|_{i+1,j,k+1/2}^{n}-E_z\Big|_{i,j,k+1/2}^{n}\right)\end{aligned} \tag{9}$$

For other sub-steps, field components, equations and computational processes similar to (8), (9) can be obtained.

In order to investigate the computational requirements of E-SSCN6-FDTD method, and compare with other unconditionally stable FDTD methods, let us determine the flops count taking into account the number of multiplication/divisions (M/D) and additions/subtractions (A/S) required for one complete time step [36]. Table 1 lists the number of arithmetic operations and tri-diagonal matrices for some unconditionally-stable FDTD methods. The count is based on the right-hand sides of their respective implicit and explicit equations using central difference operators. For simplicity, the source terms have been excluded and the numbers of electric and magnetic field components in all directions have been taken to be the same. It is also assumed that all multiplicative factors have been computed and stored.

From Table 1, it is clear that the flops count of the E-SSCN6-FDTD method has been reduced substantially compared with other unconditionally-stable FDTD methods. In particular, compared with the ADI-FDTD [21], the SS2-FDTD [38], the SS4-FDTD [44], the SS6-FDTD [45], the CNDS-FDTD [32], and the CNAFS-FDTD [31] methods, the flops count of the E-SSCN6-FDTD method is reduced by 29.4%, 33.3%, 50%, 66.7%, 38.5%, and 20%, respectively. Therefore, the computational requirement of the E-SSCN6-FDTD method is then less than those of other unconditionally-stable FDTD methods. Apart from arithmetic operations, the for-loops overhead incurred in most

Table 1. Number of arithmetic operations and tri-diagonal matrices.

Method		FDTD	ADI-FDTD [21]	LOD-FDTD [51]	SS2-FDTD [38]	SS4-FDTD [44]	SS6-FDTD [45]	CNDS-FDTD [32]	CNAFS-FDTD [31]	E-SSCN6-FDTD
Number of tri-diagonal matrices		0	6	6	9	12	18	6	9	6
Implicit	M/D	0	18	18	27	36	54	21	15	18
	A/S	0	48	24	36	48	72	66	45	24
Explicit	M/D	21	12	6	9	12	18	6	6	6
	A/S	12	24	24	36	48	72	24	24	24
Total	M/D	21	30	24	36	48	72	27	21	24
	A/S	12	72	48	72	96	144	90	69	48
	M/D + A/S	33	102	72	108	144	216	117	90	72
For-loops		6	12	12	18	24	36	10	12	12

programming languages should also be considered (cf. Table 1). Each for-loop is to perform the entire sweep along x, y, and z directions for one field component. The number of for-loops of the E-SSCN6-FDTD method is less than other unconditionally-stable FDTD methods.

Though the E-SSCN6-FDTD method and the SS6-FDTD method [45] have six sub-steps, there are some differences between two methods. For the E-SSCN6-FDTD method, at each sub-step, only one electric field component and one magnetic field component are calculated, and at one complete time step, all the electromagnetic field components are calculated for two times. However, for the SS6-FDTD method, at each sub-step, three electric field components and three magnetic field components are calculated, and at one complete time step, all the electromagnetic field components are calculated for six times. From Table 1, compared to the SS6-FDTD method, the E-SSCN6-FDTD method has flops counts reduction from 216 to 72, and has for-loops reduction from 36 to 12.

From Table 1, it can be seen that there are some commonness between the E-SSCN6-FDTD method and the LOD-FDTD method. In particular, the flop counts of two methods are 72, and the numbers of for-loops of two methods are 12. Moreover, for two methods, all the electromagnetic field components are calculated for two times. However, there also has the difference between the E-SSCN6-FDTD method and the LOD-FDTD method. Specially, in the LOD-FDTD method, at each sub-step, there are three different spatial derivatives calculated along the x, y, and z directions, and all the electromagnetic field components are calculated for one time. Nevertheless, in the E-SSCN6-FDTD method, at each sub-step, there is only one spatial derivatives along the x, or y, or z direction, and only one electric field component and one magnetic field component are calculated, which makes the form of the equations becoming concision, regularity and symmetry.

3. NUMERICAL STABILITY ANALYSIS

By using the Fourier method, assuming k_x, k_y, and k_z to be the spatial frequencies along the x, y, and z directions, the field components in spectral domain at the nth time step can be denoted as

$$U\,|_{I,J,K}^{n} = U^n e^{-j(k_x I\Delta x + k_y J\Delta y + k_z K\Delta z)} \tag{10}$$

By substituting (10) into (6a)–(6f), the following equation can be generated

$$U^{n+1} = [\Lambda_6]\,[\Lambda_5]\,[\Lambda_4]\,[\Lambda_3]\,[\Lambda_2]\,[\Lambda_1]\,U^n = [\Lambda]\,U^n \tag{11}$$

where $[\Lambda_i]$ $(i = 1 \sim 6)$ are the growth matrices of the sub-steps, and $[\Lambda]$ is the growth matrix.

$$\frac{\partial}{\partial\alpha}=jP_\alpha,\ \ P_\alpha=-2\frac{1}{\Delta\alpha}\sin\left(\frac{1}{2}k_\alpha\Delta\alpha\right),\ \ b=\Delta t/(2\varepsilon),\ \ d=\Delta t/(2\mu),$$

$$A_\alpha=1+bdC_\alpha^2P_\alpha^2,\quad B_\alpha=1-bdC_\alpha^2P_\alpha^2,\quad \alpha=x,y,z$$

$$[\Lambda]=\begin{bmatrix}
\frac{B_yB_z}{A_yA_z} & 0 & \frac{4C_xC_zbdP_xP_z}{A_xA_z} & 0 \\
\frac{4C_xC_ybdP_xP_y}{A_xA_y} & \frac{B_xB_z}{A_xA_z} & 0 & \frac{2jC_zbP_zB_x}{A_xA_z} \\
0 & \frac{4C_yC_zbdP_yP_z}{A_yA_z} & \frac{B_xB_y}{A_xA_y} & \frac{-2jC_ybP_yB_z}{A_yA_z} \\
0 & \frac{2jC_zdP_zB_y}{A_yA_z} & \frac{-2jC_ydP_yB_x}{A_xA_y} & \frac{B_yB_z}{A_yA_z} \\
\frac{-2jC_zdP_zB_y}{A_zA_y} & 0 & \frac{2jC_xdP_xB_z}{A_zA_x} & 0 \\
\frac{2jC_ydP_yB_x}{A_xA_y} & \frac{-2jC_xdP_xB_z}{A_xA_z} & 0 & \frac{4C_xpbdP_xP_z}{A_xA_z} \\
\frac{-2jC_zbP_zB_x}{A_xA_z} & \frac{2jC_ybP_yB_z}{A_zA_y} \\
0 & \frac{-2jC_xbP_xB_y}{A_xA_y} \\
\frac{2jC_xbP_xB_y}{A_xA_y} & 0 \\
\frac{4C_xC_ybdP_xP_y}{A_xA_y} & 0 \\
\frac{B_xB_z}{A_xA_z} & \frac{4C_yC_zbdP_yP_z}{A_yA_z} \\
0 & \frac{B_xB_y}{A_xA_y}
\end{bmatrix} \tag{12}$$

$$[\Lambda_1]=\begin{bmatrix}
1 & 0 & 0 & 0 & 0 & 0 \\
0 & 1 & 0 & 0 & 0 & 0 \\
0 & 0 & \frac{B_x}{A_x} & 0 & \frac{2jC_xbP_x}{A_x} & 0 \\
0 & 0 & 0 & 1 & 0 & 0 \\
0 & 0 & \frac{2jC_xdP_x}{A_x} & 0 & \frac{B_x}{A_x} & 0 \\
0 & 0 & 0 & 0 & 0 & 1
\end{bmatrix}\quad [\Lambda_2]=\begin{bmatrix}
\frac{B_y}{A_y} & 0 & 0 & 0 & 0 & \frac{2jC_ybP_y}{A_y} \\
0 & 1 & 0 & 0 & 0 & 0 \\
0 & 0 & 1 & 0 & 0 & 0 \\
0 & 0 & 0 & 1 & 0 & 0 \\
0 & 0 & 0 & 0 & 1 & 0 \\
\frac{2jC_ydP_y}{A_y} & 0 & 0 & 0 & 0 & \frac{B_y}{A_y}
\end{bmatrix}$$

$$[\Lambda_3]=\begin{bmatrix}
1 & 0 & 0 & 0 & 0 & 0 \\
0 & \frac{B_z}{A_z} & 0 & \frac{2jC_zbP_z}{A_z} & 0 & 0 \\
0 & 0 & 1 & 0 & 0 & 0 \\
0 & \frac{2jC_zdP_z}{A_z} & 0 & \frac{B_z}{A_z} & 0 & 0 \\
0 & 0 & 0 & 0 & 1 & 0 \\
0 & 0 & 0 & 0 & 0 & 1
\end{bmatrix}\quad [\Lambda_4]=\begin{bmatrix}
1 & 0 & 0 & 0 & 0 \\
0 & \frac{B_x}{A_x} & 0 & 0 & \frac{-2jC_xbP_x}{A_x} \\
0 & 0 & 1 & 0 & 0 \\
0 & 0 & 0 & 1 & 0 \\
0 & 0 & 0 & 0 & 1 \\
0 & \frac{-2jC_xdP_x}{A_x} & 0 & 0 & \frac{B_x}{A_x}
\end{bmatrix} \tag{13}$$

$$[\Lambda_5]=\begin{bmatrix} 1 & 0 & 0 & 0 & 0 & 0 \\ 0 & 1 & 0 & 0 & 0 & 0 \\ 0 & 0 & \frac{B_y}{A_y} & \frac{-2jC_y bP_y}{A_y} & 0 & 0 \\ 0 & 0 & \frac{-2jC_y dP_y}{A_y} & \frac{B_y}{A_y} & 0 & 0 \\ 0 & 0 & 0 & 0 & 1 & 0 \\ 0 & 0 & 0 & 0 & 0 & 1 \end{bmatrix} [\Lambda_6]=\begin{bmatrix} \frac{B_z}{A_z} & 0 & 0 & 0 & \frac{-2jC_z bP_z}{A_z} & 0 \\ 0 & 1 & 0 & 0 & 0 & 0 \\ 0 & 0 & 1 & 0 & 0 & 0 \\ 0 & 0 & 0 & 1 & 0 & 0 \\ \frac{-2jC_z dP_z}{A_z} & 0 & 0 & 0 & \frac{B_z}{A_z} & 0 \\ 0 & 0 & 0 & 0 & 0 & 1 \end{bmatrix}$$

By using Maple 9.0, the eigenvalues of $[\Lambda]$ can be found, as

$$\lambda_1 = \lambda_2 = 1, \quad \lambda_3 = \lambda_5 = \lambda_4^* = \lambda_6^* = \xi + j\sqrt{1-\xi^2} \tag{14}$$

where

$$\xi = \Big(1 - bd\Big(C_x^2P_x^2 + C_y^2P_y^2 + C_z^2P_z^2\Big) - b^2d^2\Big(C_x^2C_y^2P_x^2P_y^2 + C_y^2C_z^2P_y^2P_z^2 + C_x^2C_z^2P_x^2P_z^2\Big) + b^3d^3C_x^2C_y^2C_z^2P_x^2P_y^2P_z^2\Big) \Big/ \Big(1 + bd\Big(C_x^2P_x^2 + C_y^2P_y^2 + C_z^2P_z^2\Big) + b^2d^2\Big(C_x^2C_y^2P_x^2P_y^2 + C_y^2C_z^2P_y^2P_z^2 + C_x^2C_z^2P_x^2P_z^2\Big) + b^3d^3C_x^2C_y^2C_z^2P_x^2P_y^2P_z^2\Big) \tag{15}$$

Since $|\lambda_1| = |\lambda_2| = |\lambda_3| = |\lambda_4| = |\lambda_5| = |\lambda_6| = 1$, we can conclude that the E-SSCN6-FDTD method is unconditionally stable.

4. NUMERICAL DISPERSION ANALYSIS

Assume the field to be a monochromatic wave with angular frequency ω

$$E_\alpha^n = E_\alpha e^{j\omega\Delta tn},\ H_\alpha^n = H_\alpha e^{j\omega\Delta tn},\ \alpha = x,\ y,\ z \tag{16}$$

Then, (11) can be expressed as

$$\left(e^{j\omega\Delta t}[I] - [\Lambda]\right) U^n = \mathbf{0} \tag{17}$$

where U^n is related to the initial field vector U^0 and defined by

$$U^n = U^\circ e^{j\omega\Delta tn} \tag{18}$$

For a nontrivial solution of (17), the determinant of the coefficient matrix should be zero as follows

$$\det\left(e^{j\omega\Delta t}[I] - [\Lambda]\right) = 0 \tag{19}$$

With reference to the eigenvalues of $[\Lambda]$ above, the dispersion relationship of the proposed scheme can be deduced in (20).

$$\tan^2(\omega\Delta t/2) = (1-\xi)/(1+\xi) \tag{20}$$

5. CONTROLLING PARAMETERS AND DISCUSSIONS ON NUMERICAL DISPERSION PERFORMANCES

In this section, the processes of determination of the controlling parameters are shown first, and then the dispersion characteristics of the proposed method are investigated based on our generalized results. Assume that a wave propagating at angle ϕ and θ is in the spherical coordinate system. Then, $k_x = k\sin\theta\cos\phi$, $k_y = k\sin\theta\sin\phi$, $k_z = k\cos\theta$. By substituting them into the dispersion relation (20), the numerical phase velocity $\tilde{v}_p = \omega/\tilde{k}$ can be solved numerically, where $\tilde{k}$ is the numerical wave number. Subsequently, the normalized numerical phase velocity error (NNPVE) is defined as $|\tilde{v}_p/v - 1| \times 100\%$, where ν is the speed of light in the medium. Note that v is used as reference to find out the NNPVE. For clarity, CFLN is used: it is defined as the ratio between the time step taken and the maximum CFL limit of the FDTD method. In addition, the cell per wavelength (CPW): $\lambda/\Delta x$, where λ is the wavelength with no numerical anisotropy. For simplicity, uniform cells are considered here ($\Delta x = \Delta y = \Delta z$).

5.1. Determination of Controlling Parameters

Our strategy is to optimize the controlling parameters such that the normalized numerical phase velocity $A = \tilde{v}_p/v$ closes to 1 in all propagation directions. The processes of controlling parameters of the E-SSCN6-FDTD method are shown as follows.

(a) Determination of the initial controlling parameter values C_{x0}, C_{y0}, and C_{z0}.

Firstly, assume $A_0 = 1$ along three axial directions. In the x direction, let $\theta = 90^\circ$, $\phi = 0^\circ$, $k_x = k$, $k_y = 0$, $k_z = 0$. Then, $P_x = -2 \times \sin(k\Delta x/2)/\Delta x = -2 \times \sin(\pi/\mathrm{CPW})/\Delta x$, $P_y = 0$, $P_z = 0$, and the (20) can be simplified as

$$\tan^2(\omega\Delta t) = bdC_x^2P_x^2 \tag{21}$$

and $A_0 = \frac{\tilde{v}_p}{v} = \frac{\mathrm{CPW}\sqrt{3}}{\pi\mathrm{CFLN}} a\tan(-C_{x0}\sqrt{bd}P_x) = 1$. Then, we can obtain $C_{x0} = \frac{\sqrt{3}\tan[1\cdot\pi\mathrm{CFLN}/(\mathrm{CPW}\sqrt{3})]}{\mathrm{CFLN}\cdot\sin(\pi/\mathrm{CPW})}$.

In the y direction, $\theta = 90^\circ$, $\phi = 90^\circ$, $k_x = 0$, $k_y = k$, $k_z = 0$. Then $P_x = 0$, $P_y = -2 \times \sin(k\Delta y/2)/\Delta y = -2 \times \sin(\pi/\mathrm{CPW})/\Delta y$, $P_z = 0$, and we can obtain $C_{y0} = \frac{\sqrt{3}\tan[1\cdot\pi\mathrm{CFLN}/(\mathrm{CPW}\sqrt{3})]}{\mathrm{CFLN}\cdot\sin(\pi/\mathrm{CPW})}$.

In the z direction, $\theta = 0^\circ$, $k_x = 0$, $k_y = 0$, $k_z = k$, $P_x = 0$, $P_y = 0$, $P_z = -2\times\sin(k\Delta z/2)/\Delta z = -2\times\sin(\pi/\mathrm{CPW})/\Delta z$, and we can obtain $C_{z0} = \frac{\sqrt{3}\tan[1\cdot\pi\mathrm{CFLN}(\mathrm{CPW}\sqrt{3})]}{\mathrm{CFLN}\cdot\sin(\pi/\mathrm{CPW})}$.

(b) By sweeping the wave propagation angle θ and ϕ from 0° to 90°, the maximum value $A_{\max}$ at θ_m and ϕ_m can be generated.

(c) The maximum deviation of A from 1 is $Q = (A_{\max} - 1)$.

(d) Setting $A = 1 - Q/2$ along axial directions, which can be ensured that the corrected normalized phase velocity has its minimum in all propagation directions.

(e) The corrected controlling parameter values C_x, C_y, and C_z are obtained, as shown in (22).

$$C_x = C_y = C_z = \frac{\sqrt{3}\tan\left[A\pi\text{CFLN}/\left(\text{CPW}\sqrt{3}\right)\right]}{\text{CFLN}\cdot\sin\left(\pi/\text{CPW}\right)} \tag{22}$$

When CFLN = 5 and CPW = 20, the processes of controlling parameters of the E-SSCN6-FDTD method are shown as in Table 2. From Table 2, it can be observed that the values of C_x, C_y, and C_z are equal because uniform cells are used.

5.2. Numerical Dispersion Characteristics

In this subsection, to verify the superiority of the E-SSCN6-FDTD method, the numerical dispersion characteristics of the E-SSCN6-FDTD method are investigated, and compared with other unconditionally stable FDTD methods, i.e., the SSCN6-FDTD method, the CNDS-FDTD method, the CNAFS-FDTD method, and the LOD-FDTD method. Before the descriptions, two notations are introduced for clarity. The maximum dispersion error is defined as $\max\left[|\tilde{v}_p(\theta,\phi)/v - 1| \times 100\%|_{\phi=0^\circ\sim90^\circ}^{\theta=0^\circ\sim90^\circ}\right]$, and the anisotropic error can be defined as

$$\left[\max\tilde{v}_p(\theta,\phi)|_{\phi=0^\circ\sim90^\circ}^{\theta=0^\circ\sim90^\circ} - \min\tilde{v}_p(\theta,\phi)|_{\phi=0^\circ\sim90^\circ}^{\theta=0^\circ\sim90^\circ}\right]/\min\tilde{v}_p(\theta,\phi)|_{\phi=0^\circ\sim90^\circ}^{\theta=0^\circ\sim90^\circ} \times 100\%.$$

Figure 1 shows the normalized numerical phase velocity errors (NNPVEs) versus wave propagation angle ϕ with CFLN = 5, CPW = 20, $\theta = 45^\circ$ and 90° for five FDTD methods. As can be seen from Fig. 1,

Table 2. The processes of controlling parameters of the E-SSCN6-FDTD method with CFLN = 5, CPW = 20.

	E-SSCN6-FDTD
the Initial value A_0	1
The initial controlling parameter value $C_{x0} = C_{y0} = C_{z0}$	1.079120
Maximum value $A_{\max}$	1.035861
The corrected value A	0.982070
The corrected controlling parameter value $C_x = C_y = C_z$	1.056928

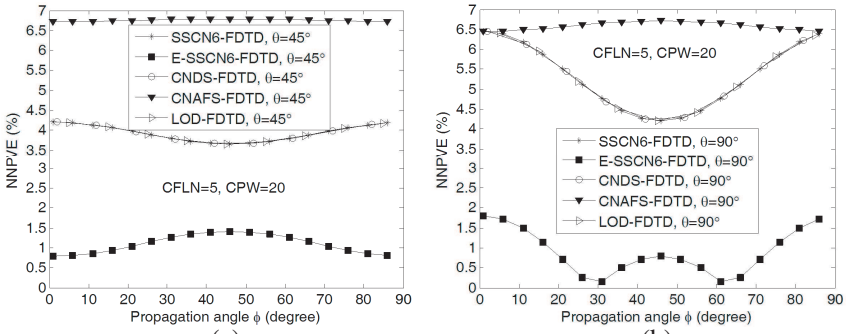

Figure 1. Normalized numerical phase velocity errors (NNPVEs) versus wave propagation angle ϕ with CFLN = 5 and CPW = 20 for five FDTD methods. (a) $\theta = 45°$. (b) $\theta = 90°$.

the NNPVE of the E-SSCN6-FDTD method is lower than those of the SSCN6-FDTD method, the CNDS-FDTD method, the LOD-FDTD method, and the CNAFS-FDTD method. Specifically, for $\theta = 45°$, $\phi = 45°$, the NNPVEs of the SSCN6-FDTD method, the LOD-FDTD method and the CNDS-FDTD method are 3.7%, and the NNPVE of the CNAFS-FDTD method is 6.8%. However, the NNPVE of the E-SSCN6-FDTD method is 1.4%, which is lower than other four FDTD methods.

Figure 2 shows the NNPVEs versus ϕ and θ with CFLN = 5 and CPW = 20 for five FDTD methods. From Fig. 2, the NNPVE of the E-SSCN6-FDTD method is lower than those of other four FDTD methods for arbitrary ϕ and θ. In particular, the maximum NNPVE of the E-SSCN6-FDTD method is 3%, whereas the maximum NNPVEs of the SSCN6-FDTD method, the CNDS-FDTD method, and the LOD-FDTD method are 6.5%.

Figure 3 shows the NNPVEs versus wave propagation angle ϕ with $\theta = 45°$, CPW = 20 and CFLN = 1, 3, 5 for two SSCN6-FDTD methods. As can be seen from Fig. 3, the NNPVEs of two SSCN6-FDTD methods increase as CFLN increases. However, the increase of the NNPVE of the E-SSCN6-FDTD method is much less pronounced than that of the SSCN6-FDTD method. For instance, with CFLN = 5 and $\phi = 45°$, the NNPVE of the E-SSCN6-FDTD method is reduced by more than 64% in comparison with the SSCN6-FDTD method. Furthermore, the NNPVE of the E-SSCN6-FDTD method with CFLN = 5 is also less than that of the SSCN6-FDTD method with CFLN = 3.

Figure 4 shows the maximum dispersion errors versus CFLN

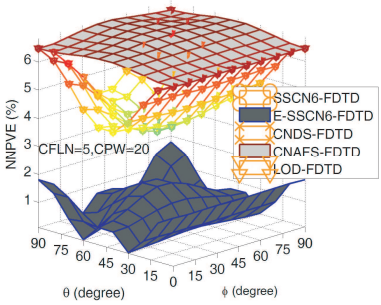

Figure 2. NNPVEs versus ϕ and θ with CFLN = 5 and CPW = 20 for five FDTD methods.

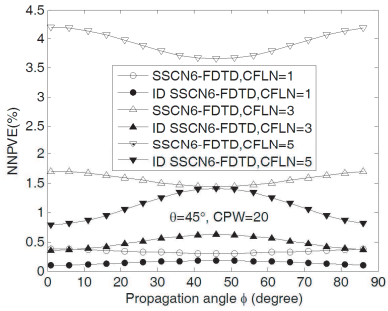

Figure 3. NNPVEs versus wave propagation angle ϕ with $\theta = 45°$, CPW = 20 and CFLN = 1, 3, 5 for two SSCN6-FDTD methods.

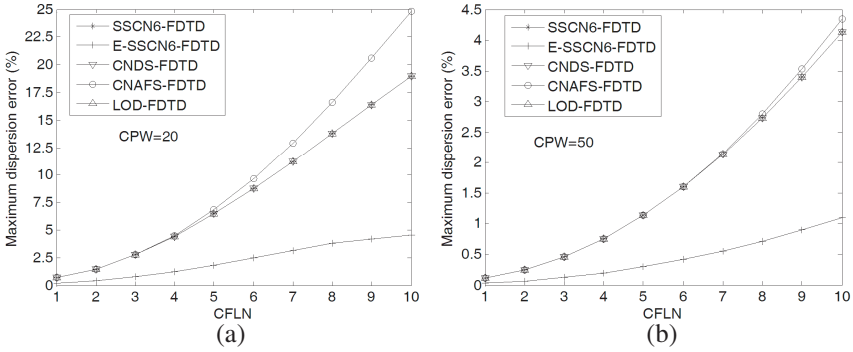

Figure 4. Maximum dispersion errors versus CFLN for five FDTD methods. (a) CPW = 20. (b) CPW = 50.

with CPW = 20 and CPW = 50 for five FDTD methods. As can be seen from Fig. 4, the maximum dispersion errors of five FDTD methods increase as CFLN increases. However, the increase of the maximum dispersion error of the E-SSCN6-FDTD method is much less pronounced than those of other FDTD methods. For instance, with CFLN = 10 and CPW = 50, the maximum dispersion errors of the SSCN6-FDTD method, the CNDS-FDTD method, and the LOD-FDTD methods are 4.13%, and the maximum dispersion error of the CNAFS-FDTD method is 4.35%. However, the maximum dispersion error of the E-SSCN6-FDTD method is 1.1%, which is lower than those of other four FDTD methods. On the other hand, with CFLN = 5 and CPW = 50, the maximum dispersion errors of the SSCN6-FDTD

method, the CNDS-FDTD method, the LOD-FDTD method, and the CNAFS-FDTD method are 1.14%, which are similar to the E-SSCN6-FDTD method with CFLN = 10 and CPW = 50. Consequently, it is concluded that the E-SSCN6-FDTD method with the larger CFLN value leads to the same level of accuracy as other four FDTD methods with the smaller CFLN value. Such an improvement of the accuracy leads to other advantages, such as saving of computation time and higher computation efficiency.

Figure 5 shows the maximum dispersion errors versus CPW with CFLN = 5 and CFLN = 10 for five FDTD methods. From Fig. 5, the maximum dispersion errors of five FDTD methods decrease as CPW increases. For the same CFLN and CPW values, the maximum dispersion error of the E-SSCN6-FDTD method is lower than those of other four FDTD methods. Moreover, other four FDTD methods have the similar maximum dispersion errors. In particular, from Fig. 5(b), when CPW = 20, the maximum dispersion error of the E-SSCN6-FDTD method is 4.5%, which is similar to the maximum dispersion errors of other four FDTD methods with CPW = 40. Therefore, it is concluded that the E-SSCN6-FDTD method with the coarsest mesh leads to the same level of accuracy as other four FDTD methods with the finest mesh, leads to other advantages, such as higher computational efficiency and lower memory requirement.

Figure 6 shows the anisotropic errors versus CFLN for five FDTD methods with CPW = 20 and CPW = 50. From Fig. 6, the anisotropic errors of five FDTD methods increase as CFLN increases. In particular, the anisotropic error of the CNAFS-FDTD method is lowest among five FDTD methods, and when CPW = 20, there is

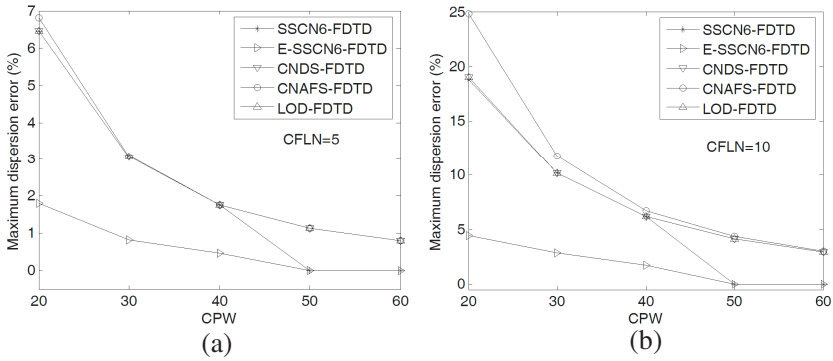

Figure 5. Maximum dispersion error versus CPW for five FDTD methods. (a) CFLN = 5. (b) CFLN = 10.

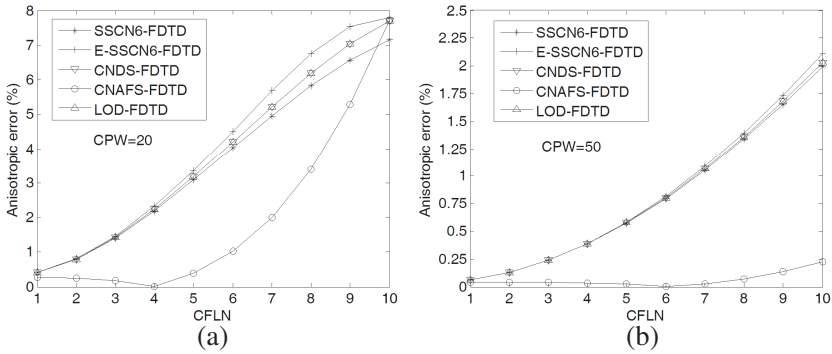

Figure 6. Anisotropic errors versus CFLN for five FDTD methods. (a) CPW= 20. (b) CPW = 50.

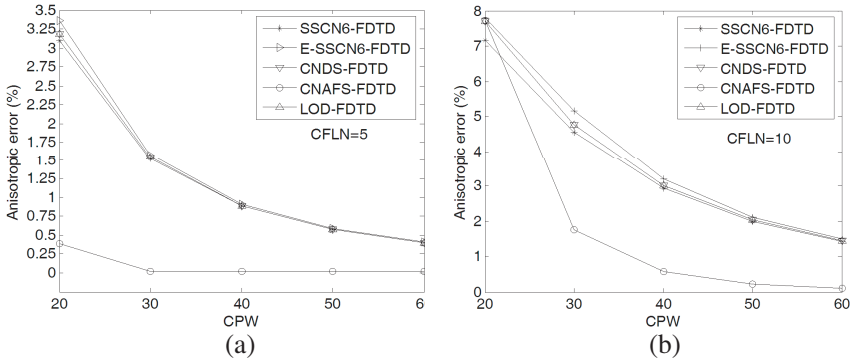

Figure 7. Anisotropic errors versus CPW for five FDTD methods. (a) CFLN= 5. (b) CFLN = 10.

a CFLN value making the anisotropic error is zero. On the other hand, the E-SSCN6-FDTD method, the SSCN6-FDTD method, the CNDS-FDTD method, and the LOD-FDTD method have the similar anisotropic errors.

Figure 7 shows the anisotropic errors versus CPW for five FDTD methods with CFLN = 5 and CFLN = 10 for five FDTD methods. As can be seen from Fig. 7, the anisotropic errors of five FDTD methods decrease as CPW increases. The E-SSCN6-FDTD method, the SSCN6-FDTD method, the CNDS-FDTD method, and the LOD-FDTD method have similar anisotropic errors. Moreover, the anisotropic error of the CNAFS-FDTD method is less than those of other four FDTD

methods, which is very pronounced in Fig. 7. Therefore, it is concluded that among the five FDTD methods, the CNAFS-FDTD method has the lowest anisotropic error.

6. NUMERICAL RESULTS

In order to verify the property of the proposed method, the SSCN6-FDTD method and the E-SSCN6-FDTD method are used to simulate a cavity of 9 mm × 6 mm × 15 mm. In addition, the cavity is filled with air and terminated with perfect electric conducting (PEC) boundaries. Moreover, a sinusoidal modulated Gaussian pulse of $\exp[-(t-t_0)^2/T^2] \times \sin\ [2\pi f_0(t-t_0)]$ is used as the excitation source, where $T = 30$ ps, $t_0 = 3 \times T$, $f_0 = 20$ GHz. The mesh size is chosen as $\Delta x = \Delta y = \Delta z = 0.60$ mm with 15 samples per wavelength at the highest frequency of the excitation source, leading to a mesh number of $15 \times 10 \times 25$. The CFLN value is 5, and the time step number is 20000. The total simulation time is selected to be 103.48 ns. The simulations are performed on a computer of Pentium IV with 2 GB RAM, and the computer program is developed with C++.

Table 3 shows the comparisons of results for two SSCN6-FDTD methods with CFLN = 5. In addition, the controlling parameters are optimized for three resonant modes, respectively. From Table 3, the relative errors of three resonant frequencies for the SSCN6-FDTD method are 2.9171%, 6.1502%, and 6.3436%, respectively. Nevertheless, the relative errors of three resonant frequencies for the E-SSCN6-FDTD method are 0.0669%, 0.9136%, and 0.2796%, respectively.

Figure 8 shows the relative errors of resonant frequencies for three modes versus CFLN for two SSCN6-FDTD methods. As can be seen from Fig. 8, for three modes, the relative errors of the SSCN6-

Table 3. Comparisons of results for two SSCN6-FDTD methods with CFLN = 5.

Resonant mode	$C_x = C_y = C_z$	E-SSCN6 -FDTD	Relative error (%)	SSCN6 -FDTD	Relative error (%)
Mode1 (TE_{101}: 19.437 GHz)	1.032947	19.45	0.0669	18.87	2.9171
Mode2 (TE_{011}: 26.926 GHz)	1.063480	26.68	0.9136	25.27	6.1502
Mode3 (TM_{111}: 30.046 GHz)	1.080693	30.13	0.2796	28.14	6.3436

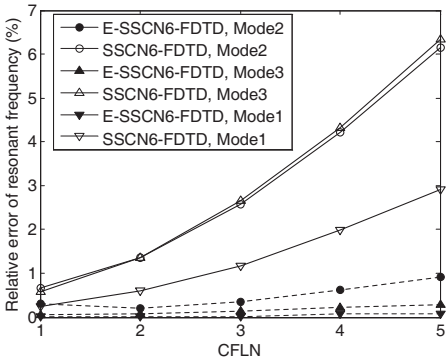

Figure 8. Relative errors of resonant frequencies for three modes versus CFLN for two SSCN6-FDTD methods.

FDTD method increase as CFLN increases. However, the increase of the relative errors of the E-SSCN6-FDTD method is less pronounced than that of the SSCN6-FDTD method. Specifically, for CFLN = 5, the relative errors for three modes of the E-SSCN6-FDTD method is also lower than 1%. Therefore, the relative errors of the E-SSCN6-FDTD method are lower than those of the SSCN6-FDTD method. In addition, the SSCN6-FDTD method requires the CPU time of 60 s and the memory requirement of 0.4892 MB, whereas the E-SSCN6-FDTD method requires the CPU time of 62 s and the memory requirement of 0.5126 MB. Consequently, the increasing in the CPU time and the memory requirement of the E-SSCN6-FDTD method can be 3.3% and 4.8% in comparisons with the SSCN6-FDTD method. The reason for the phenomenon is that adding the controlling parameters for the E-SSCN6-FDTD method, it is necessary for extra CPU time and storage. However, the increasing of the CPU time and storage are very little compared to decreasing of the relative errors. Consequently, the better accuracy and efficiency of the proposed method are achieved.

7. CONCLUSION

An efficient three-dimensional unconditionally-stable FDTD method based on the split-step scheme has been proposed, which has low numerical dispersion. In the proposed method, symmetric operator and uniform splitting have been adopted to split Maxwell's matrix into six sub-matrices, and accordingly, six sub-steps are presented. Simultaneously, three controlling parameters have been introduced to decrease the numerical dispersion error, and the dispersion characteristics of the proposed method have also been investigated.

Specifically, the NNPVE and maximum NNPVE of the E-SSCN6-FDTD method are lower than those of the SSCN6-FDTD method. Furthermore, numerical results have been presented. The relative errors of the E-SSCN6-FDTD method can be lower than those of the SSCN6-FDTD method. Therefore, the better efficiency of the E-SSCN6-FDTD method has been achieved.

ACKNOWLEDGMENT

This work is supported by the State Key Laboratory of Millimeter Waves (Southeast University, K201102).

REFERENCES

1. Yee, K. S., "Numerical solution of initial boundary value problems involving Maxwell's equations in isotropic media," *IEEE Trans. on Antennas Propag.*, Vol. 14, No. 3, 302–307, May 1966.
2. Khajehpour, A. and S. A. Mirtaheri, "Analysis of pyramid EM wave absorber by FDTD method and comparing with capacitance and homogenization methods," *Progress In Electromagnetics Research Letters*, Vol. 3, 123–131, 2008.
3. Mohammad Amjadi, S. and M. Soleimani, "Design of band-pass waveguide filter using frequency selective surfaces loaded with surface mount capacitors based on split-field update FDTD method," *Progress In Electromagnetics Research B*, Vol. 3, 271–281, 2008.
4. Ali, M. and S. Sanyal, "FDTD analysis of rectangular waveguide in receiving mode as emi sensors," *Progress In Electromagnetics Research B*, Vol. 2, 291–303, 2008.
5. Su, D., D. M. Fu, and Z. H. Chen, "Numerical modeling of active devices characterized by measured S-parameters in FDTD," *Progress In Electromagnetics Research*, Vol. 80, 381–392, 2008.
6. Wang, M.-Y., J. Xu, J. Wu, B. Wei, H.-L. Li, T. Xu, and D.-B. Ge, "FDTD study on wave propagation in layered structures with biaxial anisotropic metamaterials," *Progress In Electromagnetics Research*, Vol. 81, 253–265, 2008.
7. Liu, Y., Z. Liang, and Z. Yang, "Computation of electromagnetic dosimetry for human body using parallel FDTD algorithm combined with interpolation technique," *Progress In Electromagnetics Research*, Vol. 82, 95–107, 2008.
8. Li, J., L.-X. Guo, and H. Zeng, "FDTD method investigation on

the polarimetric scattering from 2-D rough surface," *Progress In Electromagnetics Research*, Vol. 101, 173–188, 2010.

9. Izadi, M., M. Z. A. Ab Kadir, C. Gomes, and W. F. W. Ahmad, "An analytical second-FDTD method for evaluation of electric and magnetic fields at intermediate distances from lightning channel," *Progress In Electromagnetics Research*, Vol. 110, 329–352, 2010.
10. Lee, K. H., I. Ahmed, R. S. M. Goh, E. H. Khoo, E. P. Li, and T. G. G. Hung, "Implementation of the FDTD method based on Lorentz-Drude dispersive model on GPU for plasmonics applications," *Progress In Electromagnetics Research*, Vol. 116, 441–456, 2011.
11. Izadi, M., M. Z. A. A. Kadir, and C. Gomes, "Evaluation of electromagnetic fields associated with inclined lightning channel using second order FDTD-Hybrid methods," *Progress In Electromagnetics Research*, Vol. 117, 209–236, 2011.
12. Luo, S. and Z. D. Chen, "An efficient model FDTD for absorbing boundary conditions and incident wave generator in waveguide structures," *Progress In Electromagnetics Research*, Vol. 68, 229–246, 2007.
13. Xiao, S.-Q., B.-Z. Wang, P. Du, and Z. Shao, "An enhanced FDTD model for complex lumped circuits," *Progress In Electromagnetics Research*, Vol. 76, 485–495, 2007.
14. Liu, Y., Z. Liang, and Z. Yang, "A novel FDTD approach featuring two-level parallelization on pc cluster," *Progress In Electromagnetics Research*, Vol. 80, 393–408, 2008.
15. Xiao, S.-Q. Z. H. Shao, and B.-Z. Wang, "Application of the improved matrix type FDTD method for active antenna analysis," *Progress In Electromagnetics Research*, Vol. 100, 245–263, 2010.
16. Sirenko, K., V. Pazymin,, Y. K. Sirenko, and H. Bagci, "An FFT-accelerated FDTD scheme with exact absorbing conditions for characterizing axially symmetric resonant structures," *Progress In Electromagnetics Research*, Vol. 111, 331–364, 2011.
17. Vaccari, A., A. Cala' Lesina, L. Cristoforetti, and R. Pontalti, "Parallel implementation of a 3D subgridding FDTD algorithm for large simulations," *Progress In Electromagnetics Research*, Vol. 120, 263–292, 2011.
18. Chen, C.-Y., Q. Wu, X.-J. Bi, Y.-M. Wu, and L.-W. Li, "Characteristic analysis for FDTD based on frequency response," *Journal of Electromagnetic Waves and Application*, Vol. 24, No. 2–3, 282–292, 2010.
19. Taflove, A. and S. C. Hagness, *Computational Electrodynamics:*

the Finite-difference Time-domain Method, 2nd Edition, Artech House, Boston, MA, 2000.

20. Namiki, T., "A new FDTD algorithm based on alternating-direction implicit method," *IEEE Trans. on Microwave Theory and Tech.*, Vol. 47, No. 10, 2003–2007, Oct. 1999.
21. Zheng, F., Z. Chen, and J. Zhang, "Toward the development of a three-dimensional unconditionally stable finite-difference time-domain method," *IEEE Trans. on Microwave Theory and Tech.*, Vol. 48, No. 9, 1550–1558, Sep. 2000.
22. Wang, M. H., Z. Wang, and J. Chen, "A parameter optimized ADI-FDTD method," *IEEE Antennas Wireless Propag. Lett.*, Vol. 2, No. 1, 118–121, 2003.
23. Ahmed, I. and Z. Chen, "Dispersion-error optimized ADI-FDTD," *Proc. IEEE MTT-S Int. Microw. Symp. Dig.*, 173–176, Jun. 2006.
24. Zhao, A. P., "Improvement on the numerical dispersion of 2-D ADI-FDTD with artificial anisotropy," *IEEE Microw. Wireless Compon. Lett.*, Vol. 14, No. 6, 292–294, Jun. 2004.
25. Zheng, H. X. and K. W. Leung, "An efficient method to reduce the numerical dispersion in the ADI-FDTD," *IEEE Trans. on Microwave Theory and Tech.*, Vol. 53, No. 7, 2295–2301, Jul. 2005.
26. Zhang, Y., S. W. Lu, and J. Zhang "Reduction of numerical dispersion of 3-D higher order alternating-direction-implicit finite-difference time-domain method with artificial anisotropy," *IEEE Trans. on Microwave Theory and Tech.*, Vol. 57, No. 10, 2416–2428, Oct. 2009.
27. Kong, K.-B., S.-O. Park, and J.-S. Kim, "Stability and numerical dispersion of 3-D simplified sampling biorthogonal ADI method," *Journal of Electromagnetic Waves and Application*, Vol. 24, No. 1, 1–12, 2010.
28. Sun, G. and C. W. Trueman, "Unconditionally stable Crank-Nicolson scheme for solving the two-dimensional Maxwell's equations," *Electron. Lett.*, Vol. 39, No. 7, 595–597, Apr. 2003.
29. Sun, G. and C. W. Trueman, "Approximate Crank-Nicolson schemes for the 2-D finite-difference time-domain method for TEz waves," *IEEE Trans. on Antennas Propag.*, Vol. 52, No. 11, 2963–2972, Nov. 2004.
30. Sun, G. and C. W. Trueman, "The unconditionally-stable cycle-sweep method for 3-D FDTD," *10th Int. Antenna Technol. Appl. Electromagn. Symp./URSI Conf.*, Ottawa, ON, Canada, Jul. 20–23, 2004.
31. Sun, G. and C. W. Trueman, "Unconditionally-stable FDTD

method based on Crank-Nicolson scheme for solving three-dimensional Maxwell equations," *Electron. Lett.*, Vol. 40, No. 10, 589–590, May 2004.

32. Sun, G. and C. W. Trueman, "Efficient implementations of the Crank-Nicolson scheme for the finite-difference time-domain method," *IEEE Trans. on Microwave Theory and Tech.*, Vol. 54, No. 5, 2275–2284, May 2006.
33. Xu, K., Z. Fan, D.-Z. Ding, and R.-S. Chen, "GPU accelerated unconditionally stable Crank-Nicolson FDTD method for the analysis of three-dimensional microwave circuits," *Progress In Electromagnetics Research*, Vol. 102, 381–395, 2010.
34. Ramadan, O. and A. Y. Oztoprak, "Unconditionally-stable Crank-Nicolson wave-equation PML formulations for truncating FDTD domains," *Electrical Engineering*, Vol. 89, No. 2, 89–93, Dec. 2006.
35. Mirzavand, R., A. Abdipour, G. Moradi, and M. Movahhedi, "CFS-PML implementation for the unconditionally stable FDTD method," *Journal of Electromagnetic Waves and Application*, Vol. 25, No. 5-6, 879–888, 2011.
36. Tan, E. L., "Efficient algorithms for Crank-Nicolson-based finite-difference time-domain methods," *IEEE Trans. on Microwave Theory and Tech.*, Vol. 56, No. 2, 408–413, Feb. 2008.
37. Lee, J. and B. Fornberg, "A split step approach for the 3-D Maxwell's equations," *J. Comput. Appl. Math.*, No. 158, 485–505, Mar. 2003.
38. Lee, J. and B. Fornberg, "Some unconditionally stable time stepping methods for the 3D Maxwell's equations," *J. Comput. Appl. Math.*, No. 166, 497–523, Mar. 2004.
39. Fu, W. and E. L. Tan, "Development of split-step FDTD method with higher-order spatial accuracy," *Electron. Lett.*, Vol. 40, No. 20, 1252–1253, Sep. 2004.
40. Fu, W. and E. L. Tan, "Compact higher-order split-step FDTD method," *Electron. Lett.*, Vol. 41, No. 7, 397–399, Mar. 2005.
41. Xiao, F., "High-order accurate unconditionally-stable implicit multi-stage FDTD method," *Electron. Lett.*, Vol. 42, No. 10, 564–566, May 2006.
42. Kusaf, M. and A. Y. Oztoprak, "An unconditionally-stable split-step FDTD method for low anisotropy," *IEEE Microw. Wireless Compon. Lett.*, Vol. 18, No. 4, 224–226, Apr. 2008.
43. Chu, Q. X. and Y. D. Kong, "High-order accurate FDTD method based on split-step scheme for solving Maxwell's equations,"

Microwave. Optical. Technol. Lett., Vol. 51, No. 2, 562–565, Feb. 2009.

44. Kong, Y. D. and Q. X. Chu, "High-order split-step unconditionally-stable FDTD methods and numerical analysis," *IEEE Trans. on Antennas Propag.*, Vol. 59, No. 9, 3280–3289, Sep. 2011.
45. Xiao, F., X. H. Tang, L. Guo, and T. Wu, "High-order accurate split-step FDTD method for solution of Maxwell's equations," *Electron. Lett.*, Vol. 43, No. 2, 72–73, Jan. 2007.
46. Chu, Q. X. and Y. D. Kong, "Three new unconditionally-stable FDTD methods with high-order accuracy," *IEEE Trans. on Antennas Propag.*, Vol. 57, No. 9, 2675–2682, Sep. 2009.
47. Kong, Y. D. and Q. X. Chu, "An unconditionally-stable FDTD method based on split-step scheme for solving three-dimensional Maxwell equations," *IEEE International Conference on Microwave and Millimeter Wave Technology*, Vol. 1, 194–197, Nanjing, China, Apr. 2008.
48. Shibayama, J., M. Muraki, J. Yamauchi, and H. Nakano, "Effcient implicit FDTD algorithm based on locally one-dimensional scheme," *Electron. Lett.*, Vol. 41, No. 19, 1046–1047, Sep. 2005.
49. Do Nascimento, V. E., J. A. Cuminato, F. L. Teixeira, and B.-H. V. Borges, "Unconditionally stable finite-difference time-domain method based on the locally-one-dimensional technique," *Proc. XXII Simpósio Brasileiro de Telecomunicações*, 288–291, Campinas, SP, Brazil, Sep. 2005.
50. Ahmed, I., E. K. Chua, E. P. Li, and Z. Chen, "Development of the three-dimensional unconditionally-stable LOD-FDTD method," *IEEE Trans. on Antennas Propag.*, Vol. 56, No. 11, 3596–3600, Nov. 2008.
51. Liu, Q. F., Z. Chen, and W. Y. Yin, "An arbitrary order LOD-FDTD method and its stability and numerical dispersion," *IEEE Trans. on Antennas Propag.*, Vol. 57, No. 8, 2409–2417, Aug. 2009.
52. Tay, W. C. and E. L. Tan, "Implementations of PMC and PEC boundary conditions for efficient fundamental ADI and LOD-FDTD," *Journal of Electromagnetic Waves and Application*, Vol. 24, No. 4, 565–573, 2010.